Joint nonlinear electrical equalization in coherent optical PDM DFT-spread-OFDM systems

Zhiyuan Huang (黄志远), Fan Zhang (张 帆)*, and Zhangyuan Chen (陈章渊)**

State Key Laboratory of Advanced Optical Communication Systems and Networks, Peking University, Beijing 100871, China

**Corresponding author: fzhang@pku.edu.cn; **corresponding author: chenzhy@pku.edu.cn*

Received December 20, 2012; accepted February 25, 2013; posted online May 30, 2013

We propose a joint nonlinear electrical equalization approach in coherent optical discrete-Fourier-transform spread orthogonal-frequency-division-multiplexing (DFT-spread-OFDM) systems with polarization division multiplexing (PDM). This method is based on an adaptive Volterra series expansion for nonlinear distortions of two orthogonal polarizations. The nonlinear electrical equalization is validated through numerical simulation of 100-Gb/s quadrature phase shift keying and 200-Gb/s 16 quadrature amplitude modulation PDM DFT-spread-OFDM systems.

OCIS codes: 060.4370, 060.4510, 060.4230.

doi: 10.3788/COL201311.060601.

The demand for high-capacity optical transmission has resulted in the rapid development of coherent optical (CO) systems. Linear impairments, such as fiber chromatic dispersion (CD) and polarization mode dispersion (PMD), can be compensated in principle for CO communication. Thus, fiber capacity is ultimately limited by nonlinearity and amplified spontaneous emission (ASE) in optical amplifiers. Given that the ASE noise corresponds to the well known Shannon limit and cannot be eliminated, fiber nonlinearity remains one of the dominant impairments that degrade system performance and capacity[1−3]. Numerous nonlinear mitigation techniques, such as digital back-propagation (BP)[4], adaptive nonlinear electrical equalization (NLEE) based on Volterra series[5−7], and maximum-likelihood sequence estimation (MLSE)[8], have been studied. BP is sensitive to the sampling and processing rate, whereas the MLSE cannot be easily adapted to different systems[9]. Thus, NLEE has been applied because it is more adaptive to compensate the nonlinearity from optical fiber Kerr effects. Gao *et al.* first demonstrated the validity of Volterra-based NLEE in 10-Gbaud/s non-return-to-zero (NRZ)-quadrature phase shift keying (QPSK) system for a 1 600-km simulation and a 400-km experiment[5,6]. Pan *et al.* extended the NLEE to a 14-Gbaud/s 16 quadrature amplitude modulation (16QAM) system with 1 200-km simulation and a 28-Gbaud/s QPSK system with a 1 600-km simulation[10]. Weidenfeld *et al.* applied the NLEE to a long-haul orthogonal-frequency-division-multiplexing (OFDM) system over a of 2 000-km simulation[11]. Pan *et al.* discussed the position of the NLEE before and after transmission in the simulation of a 100-Gb/s CO-OFDM system[12].

The aforementioned studies mainly focused on the nonlinear equalization in single polarization system. However, intra-channel nonlinear distortions also result from interactions from the orthogonal polarization (OP) for a dual-polarization (DP) system. Dou *et al.* proposed a predistortion method in a 43-Gb/s DP-QPSK system with joint equalization of two polarizations[13]. Liu *et al.* introduced a frequency-domain Volterra series transfer function method in a 1 000-km simulation for a 256-Gb/s DP-16QAM transmission system[9]. However, both methods are relatively sensitive to the values of the optical fiber parameters and less adaptive to be implemented. We applied the joint equalization into NLEE and implemented it into a discrete-Fourier-transform spread OFDM (DFT-spread-OFDM) system. The DFT-spread-OFDM system has a lower peak-to-average power ratio (PAPR) and better nonlinear tolerance compared with the conventional OFDM system. Moreover, the NLEE method can realize blind equalization because it does not require prior knowledge of the fiber link parameters to calculate the Volterra kernels. The kernels are adaptively determined using recursive least square (RLS) method. This advantage provides enough flexibility when signals are routed differently in optical networks.

Nonlinear optical propagation in fiber systems are well modeled by the Volterra series expansion[14]. The solution of the third-order nonlinear distortion for an input signal $A(n)$ can be written as

$$\Delta A(n) = \sum_{l=-N}^{N} \sum_{m=l}^{N} \sum_{k=m}^{N} H_{l,\,m,\,k} A(l) A(m) A^*(k), \quad (1)$$

where l, m, n, and k are time indices; $H_{l,\,m,\,k}$ refers to the third-order Volterra kernels for the nonlinear transfer function. The intrachannel nonlinear impairments of polarization x also come from the interactions with polarization y for a DP system (Fig. 1).

The solutions of $\Delta A_x(n)$ and $\Delta A_y(n)$ are shown in Fig. 1 and expressed as

$$\Delta A_x(n) = \sum_{l=-N}^{N} \sum_{k=l}^{N} A_x(n+k-l) \cdot [A_x(l) A_x^*(k) + A_y(l) A_y^*(k)] H_{l,k,n+k-l}, \quad (2)$$

$$\Delta A_y(n) = \sum_{l=-N}^{N} \sum_{k=l}^{N} A_y(n+k-l) \cdot [A_x(l) A_x^*(k) + A_y(l) A_y^*(k)] H_{l,\,k,\,n+k-l}. \quad (3)$$

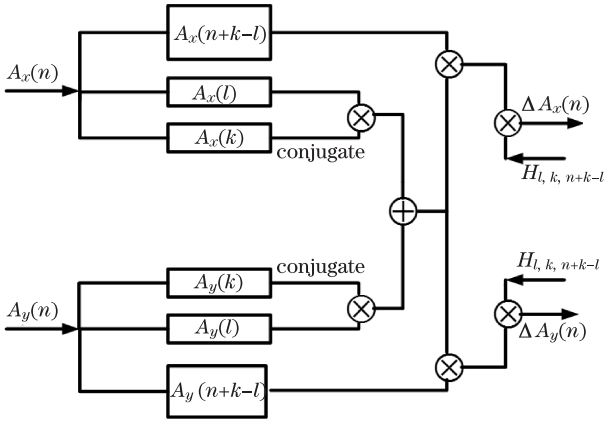

Fig. 1. Diagram for the calculation of intrachannel nonlinearity of input signals.

Considering the different values of l and k, we can further express the equation for $\Delta A_x(n)$ as

$$\begin{aligned}\Delta A_x(n) = &\sum_{l=-N}^{N} H_l[A_x(l)(|A_x(l)|^2+|A_y(l)|^2)]\\ &+\sum_{l=-N}^{N}\sum_{k=l}^{N} H_{l,\,n+k-l}[A_x(l)(|A_x(n+k-l)|^2\\ &+|A_y(n+k-l)|^2)]\\ &+\sum_{l=-N}^{N}\sum_{k=l}^{N} H_{l,\,n+k-l}[A_x(n+k-l)|A_x(l)|^2\\ &+A_x(l)A_y(n+k-l)A_y^*(l)]\\ &+\sum_{l=-N}^{N}\sum_{k=l}^{N} H_{l,\,k,\,n+k-l}[A_x(l)A_x(n+k-l)A_x^*(k)\\ &+A_x(l)A_y(n+k-l)A_y^*(k)]. \qquad (4)\end{aligned}$$

Equation (4) provides a general closed-form solution of the intra-channel nonlinearity. $\Delta A_y(n)$ can be expressed similarly. The self-phase modulation is considered as the first term, the intra-channel cross-phase modulation as the second and third terms, and the intra-channel four-wave-mixing as the last term. Note that only those pulses with indices satisfying $l+m-k=n$ could induce sizeable distortions to the system[6]. Thus, we replace m with $n+k-l$ in Fig. 1 and Eqs. (2)–(4). All Volterra kernels in Eq. (4) can be calculated using the RLS method.

Figure 2 shows the diagram for RLS. We can obtain the Volterra kernels by minimizing the cost function $e(n)[e(n)=A(n)-d(n)]$. We need to send a short training sequence to obtain the expected $d(n)$ signal. For instance, a length of 200 for the training sequence should be enough for a symbol with a fast Fourier transform (FFT) size of 4096, and no more training sequences are required for the following symbols. The expected signal can be generated recursively. This method does not require prior knowledge of the fiber link parameters and can eventually provide more flexibility for the transmission system.

The number of operations per symbol is proportional to N^2 in the scheme of conventional Volterra-based nonlinear equalizers, where N refers to the total term number of the equalizers[15]. Although nonlinear distortions from both polarizations are considered, the basic structure of our NLEE is still Volterra-based. Therefore, the computation complexity is at the same level as the conventional nonlinear equalizers, which is also proportional to N^2. Notably, the value of N is decided by the tap length of NLEE, which must be long enough to consider the nonlinear inter-symbol interference between the overlapped optical pulses. Therefore, the tap length is related to the accumulated chromatic dispersion in the system. In particular, the tap length in our system has been optimized to 15. Thus, N is equal to 88 and approximately $1.2e^4$ multiplications and $1.2e^4$ additions are involved in computation.

Figure 3 illustrates the digital signal processing (DSP) block diagrams for the DFT-spread-OFDM scheme. At the encoder, the transmitted binary data are mapped into QAM or phase shift keying (PSK) signals before they are grouped into M-symbol blocks. After an M-point DFT to produce a frequency domain representation of the input symbols, the M-point DFT output is mapped to N ($N \geqslant M$) orthogonal subcarriers, followed by the N-point inverse FFT (IFFT), which transforms the subcarriers into time domain. Cyclic prefix (CP) is inserted for each block and then the data sequence is transmitted. At the decoder, the N-point DFT transforms the signal into frequency domain, and channel equalization is then performed. The equalized signal is transformed into time domain again by the M-point inverse DFT (IDFT) for decision. The DFT-spread-OFDM system has a significantly lower PAPR compared with the conventional OFDM system. Therefore, it suffers less nonlinear impairment and enhances the nonlinear tolerance of the system[16]. The DFT-spread-OFDM system could be more flexible than the traditional single-carrier systems because it utilizes frequency-domain equalization and subcarrier mapping.

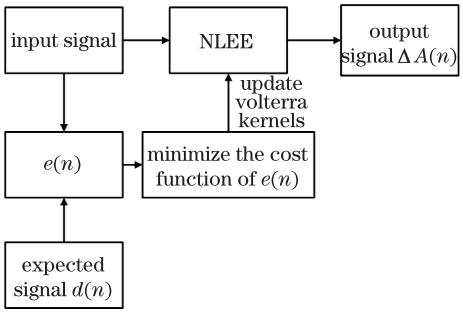

Fig. 2. Diagram for the RLS method.

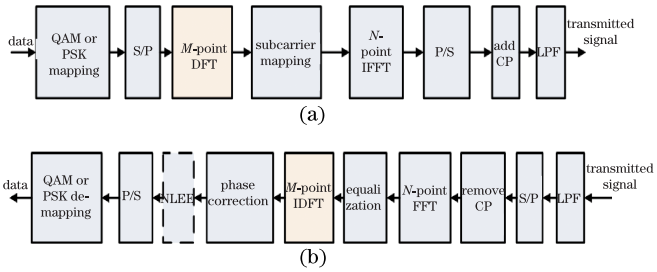

Fig. 3. DSP block diagrams for (a) encoder (b) decoder in DFT-spread-OFDM systems. S/P: serial/paralle; P/S: parallel/serial; LPF: low-pass filter.

Furthermore, the orthogonality of the system can be guaranteed to be similar to the OFDM system because of the application of DFT processing[17].

Figure 3(b) shows the implementation of the NLEE method. We assume that N=4 096, M=3 424, and CP=240. The sampling rate is chosen to be 37 GS/s. A net bit rate of 100 Gb/s for QPSK and 200 Gb/s for 16QAM will be obtained when we set a preamble ratio to 2.44% and a redundancy ratio to 12% to include overhead for Ethernet (64B/66B) and forward error correction (FEC) coding[18].

The simulations are conducted via commercial software (VPI) Transmission Maker 8.6, VPI systems, USA. The fiber link consists of multi-span of 80-km standard single-mode fiber (SSMF) with an average loss of 20 dB each. Fiber dispersion is 17 ps/(km·nm) and fiber nonlinear coefficient is 1.32 $\mathrm{km^{-1}\cdot W^{-1}}$. An erbium-doped fiber amplifier with a noise figure of 5 dB fully compensates the fiber attenuation. Noinline CD compensation is used. The transmission length for the simulation is 4 000 km (50 × 80 km) for QPSK and 1 600 km (20 × 80 km) for 16QAM. We evaluated the system performance by comparing the required optical signal-to-noise ratio (OSNR) at a bit error rate (BER) target of 10^{-3} with and without NLEE compensation.

As mentioned above, the nonlinear effects from OP should not be neglected in the polarization division multiplexing (PDM) systems. Figsures 4 and 5 illustrate the Q-factor performance as a function of launch power. The curves denote the following: (1) square, without NLEE; (2) circle, NLEE without considering the distortions from OP; (3) triangle, NLEE with distortions from OP. The BER is converted

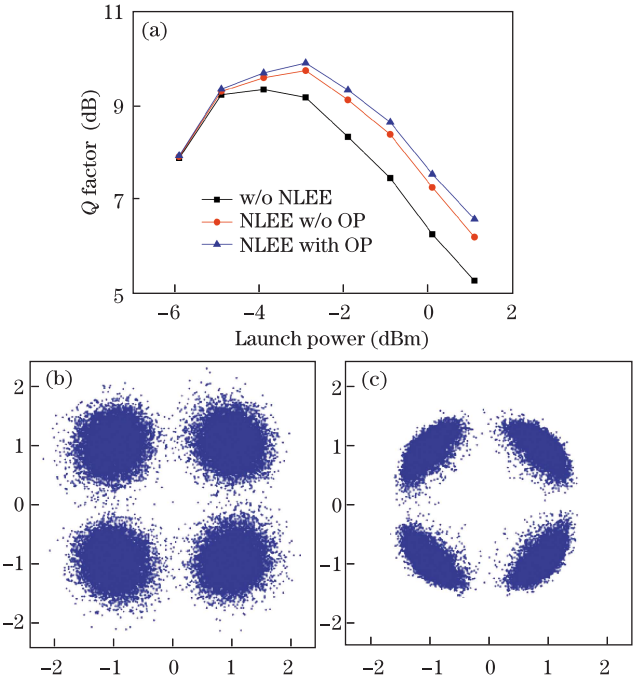

Fig. 4. (a) Q-factor performance as a function of launch power for a 100-Gb/s QPSK DFT-spread-OFDM signal transmitting over 4 000-km SSMF; constellations for QPSK signal at –3-dBm launch power (b) without and (c) with NLEE considering distortions from OP.

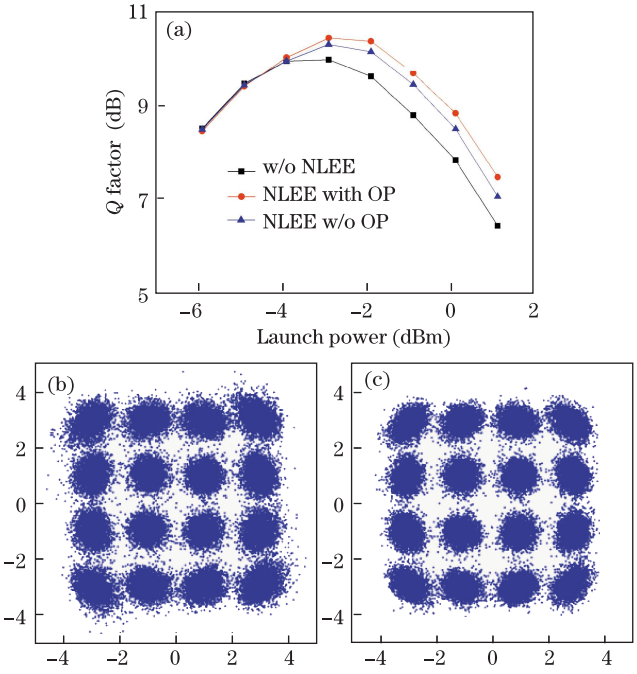

Fig. 5. (a) Q-factor performance with different launch powers for a 200-Gb/s 16QAM DFT-spread-OFDM signal transmitting over 1 600-km SSMF; constellations for 16QAM signal at –3-dBm launch power (b) without and (c) with NLEE considering distortions from OP.

to Q_{BER} in dB using the relationship $Q_{\mathrm{BER}} = 20\log\left[\sqrt{2}\mathrm{erfc}^{-1}(2\mathrm{BER})\right]$, where erfc^{-1} is the inverse complementary error function. A BER target of 10^{-3} corresponds to a Q_{BER} value of 9.8 dB. The transmission performance declines at low launch power because of decreased OSNR and at high launch power because of increased nonlinear impairments. The Q-factor for nonlinear equalization with OP reaches its maximum value with a launch power of –3 dBm when the Q improvement is 0.88 dB in QPSK system and 0.68 dB in 16QAM system. Larger improvement for the Q-factor can be observed in both the QPSK and 16QAM systems with an increase in the launch power.

Figures 6 and 7 demonstrate the required OSNRs at 10^{-3} BER target versus different launch powers. The required OSNR values corresponding to the electrical equalizations with and without nonlinear compensation remain almost the same when the launch power is less than –4 dBm. System performance clearly improves and the required OSNR reduces significantly when the launch power is increased. For instance, the required OSNR reduction is 1.1 dB at –3 dBm and 2.5 dB at –2 dBm for the QPSK system and 0.5 dB at –3 dBm and 1.8 dB at –2 dBm for the 16QAM system. We can obtain better system performance with joint nonlinear equalization, which mitigates distortions from OP. The required OSNR can be further reduced by 0.6 and 1.3 dB at –2 and –1 dBm launch powers, respectively, in the QPSK system. The reduction difference is more than 1.5 dB for nonlinear equalization with and without OP for the 16QAM system at the launch power of –1 dBm.

In conclusion, we propose the nonlinear equalization scheme in CO PDM DFT-spread-OFDM systems. The

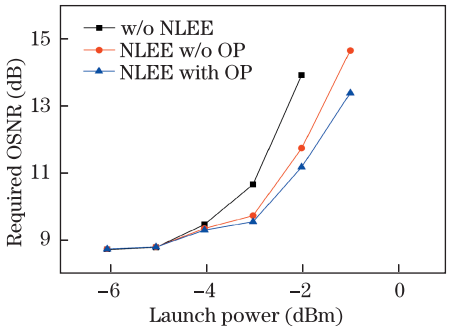

Fig. 6. Required OSNR at 10^{-3} BER versus launch power in QPSK system.

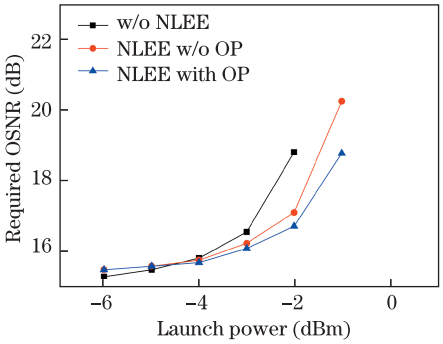

Fig. 7. Required OSNR at 10^{-3} BER versus launch power in 16QAM system.

NLEE compensation based on Volterra theory is demonstrated, and a joint equalization of nonlinear distortions from the OP in DP systems is applied. The NLEE method is validated by numerical simulation of 100-Gb/s QPSK and 200-Gb/s 16QAM PDM DFT-spread-OFDM systems. The simulation results show that NLEE application with joint equalization can significantly improve system performance at high launch power.

This work was supported by the National Natural Science Foundation of China (Nos. 61077053, 60932004, and 61275005), the National "863" Program of China (No. 2012AA011302), and the National "973" Program of China (No. 2010CB328201). This work was partially supported by the Program for New Century Excellent Talents in University.

References

1. E. Yamazaki, A. Sano, T. Kobayashi, E. Yoshida, and Y. Miyamoto, in *Proceedings of OFC 2011* OThF1 (2011).
2. C. Lin, R. Asif, M. Holtmannspoetter, and B. Schmauss, Chin. Opt. Lett. **10,** 020605 (2012).
3. Y. Hao, Y. Li, R. Wang, and W. Huang, Chin. Opt. Lett. **10,** 010701 (2012).
4. E. Ip and J. Kahn, J. Lightwave Technol. **26,** 3416 (2008).
5. Y. Gao, F. Zhang, J. Li, L. Liu, Z. Chen, L. Zhu, L. Li, and A. Xu, in *Proceedings of ECOC 2009* P9.4.7 (2009).
6. Y. Gao, F. Zhang, L. Dou, Z. Chen, and A. Xu, Opt. Commun. **282,** 2421 (2009).
7. F. Zhang, Y, Gao, Y. Luo, J. Li, L. Zhu, L. Li, Z. Chen, and A. Xu, Electron. Lett. **46,** 353 (2010).
8. N. Stojanovic, Y. Huang, F. Hauske, Y. Fang, M. Chen, C. Xie, and Q. Xiong, in *Proceedings of OFC 2011* OWW6 (2011).
9. L. Liu, L. Li, Y. Huang, K. Cui, Q. Xiong, F. Hauske, C. Xie, and Y. Cai, J. Lightwave Technol. **30,** 310 (2012).
10. Z. Pan, B. Chatelain, M. Chagnon, and D. Plant, in *Proceedings of OFC 2011* JThA40 (2011).
11. R. Weidenfeld, M. Nazarathy, R. Noe, and I. Shpantzer, in *Proceedings of OFC 2010* OTuE3 (2010).
12. J. Pan and C. Cheng, J. Lightwave Technol. **29,** 2785 (2011).
13. L. Dou, Z. Tao, L. Li, W. Yan, T. Tanimura, T. Hoshida, and J. Rasmussen, in *Proceedings of OFC 2011* OThF5 (2011).
14. K. Peddanarappagari and M. Brandt-Pearce, J. Lightwave Technol. **15,** 2232 (1997).
15. J. G. Proakis, Digital Communications, Chapter **11** (2001).
16. C. Zhao, Y. Chen, S. Zhang, J. Li, F. Zhang, L. Zhu, and Z. Chen, Opt. Express **20,** 787 (2012).
17. J. Li, S. Zhang, F. Zhang, and Z. Chen, in *Proceedings of Photonics in Switching 2010* JTuB41 (2010).
18. F. Chang, K. Onohara, and T. Mizuochi, IEEE Commun. Mag. **48,** S48 (2010).